Journal of Catalysis 269 (2010) 71–79

Contents lists available at ScienceDirect

Journal of Catalysis

journal homepage: www.elsevier.com/locate/jcat

Small-sized HZSM-5 zeolite as highly active catalyst for gas phase dehydration of glycerol to acrolein

Chun-Jiang Jia, Yong Liu, Wolfgang Schmidt, An-Hui Lu, Ferdi Schüth *

Max-Planck-Institut für Kohlenforschung, Kaiser-Wilhelm-Platz 1, 45470 Mülheim an der Ruhr, Germany

ARTICLE INFO

Article history:
Received 27 August 2009
Revised 5 October 2009
Accepted 19 October 2009
Available online 18 November 2009

Keywords:
Glycerol dehydration
Acrolein
Zeolite
HZSM-5
Particle size

ABSTRACT

The catalytic properties of nanocrystalline HZSM-5 catalysts with high Si/Al molar ratio (ca. 65) were investigated in the gas phase dehydration of aqueous glycerol. Compared with bulk HZSM-5, the small-sized catalyst exhibits greatly enhanced catalytic performance in glycerol dehydration even with very high GHSV (=1438 h^{-1}). Catalysts with different Si/Al ratios were studied, but it is difficult to separate the influence of Si/Al ratio from that of particle size. However, by varying the proton exchange degree for one mother batch of zeolite, a series of H_xNa_{1-x}ZSM-5 catalysts with same particle size and different Brønsted acid site densities was prepared. The catalytic results for this series of samples show that high density of Brønsted acid sites favors the production of acrolein. Based on these results, small-sized HZSM-5 with high aluminum content appears to be most promising for gas phase dehydration of glycerol.

1. Introduction

In recent years, the conversion of renewable resources, such as plant biomass, to produce fuels and chemicals has become an increasingly important research topic in energy-related catalysis. Glycerol is a main byproduct in biodiesel production. The increasing use of biodiesel (fatty acid methyl esters, FAME) has resulted in an increase of glycerol production and a price decline, which makes glycerol an attractive precursor molecule for producing other valuable chemicals [1–3]. Even if the initial enthusiasm over oil-plant-based FAME has decreased to some extent, due to competition with food and feed, it is expected that oil-plants growing on marginal lands, such a Jatropha, will increase in importance [4]. One of the best-known acid catalyzed reactions with glycerol is dehydration to form acrolein (as shown in Scheme 1) which is a versatile intermediate largely employed by the chemical industry for the production of acrylic acid esters, superabsorber polymers, and detergents. Various solid acid catalysts, including sulfates, phosphates, zeolites, solid phosphoric acid and others, have been tested for the dehydration of glycerol to acrolein in either gaseous or liquid phases [5–12]. Besides the solid acid catalysts, liquid acids (H_2SO_4) and salts ($ZnSO_4$) were also used as catalysts to investigate the dehydration of glycerol under sub-supercritical and supercritical conditions [13–17]. However, the production of acrolein from glycerol was not commercialized owing to its poor economics compared to a traditional production route based on the oxidation of propylene with a Bi/Mo-based multi metal oxide catalyst. Nevertheless, since both oil prices – and the related propylene prices – and glycerol prices are fluctuating strongly, the search for a more efficient catalyst for the dehydration of glycerol and the development of better process alternatives still attracts great attention.

Zeolites are crystalline microporous alumosilicates consisting of tetrahedral SiO_4 and AlO_4 units which are connected via shared oxygen sites to form open framework structures. This generates a system of pores and cavities with molecular dimensions [18–20]. Zeolite materials are widely used in applications, such as catalysis and chemical separations. The medium pore size zeolite ZSM-5 is a prominent and commercially important member of this class of materials which has found applications in a number of petrochemical processes [21,22]. HZSM-5 has also been used as catalyst for glycerol dehydration. Neher et al. carried out this reaction in liquid phase at 250–300 °C and 70 bar using HZSM-5 as the catalyst [6]. At low conversion of glycerol (15–19 mol%), they observed high selectivity (71–75 mol%) to acrolein. Chai et al. reported for gas phase dehydration (GHSV = 80 h^{-1}) with a fixed bed reactor at 315 °C, using HZSM-5 as catalyst, a relatively low glycerol conversion (23 mol%), and acrolein selectivity (52 mol%) at TOS = 9–10 h [23]. This was tentatively attributed to micropore blockage by carbon deposits during the reaction. However, no information on particle size and Si/Al ratio of the HZSM-5 catalyst was given in these two reports. Recently, Corma et al. investigated the dehydration of glycerol on zeolite-based catalyst in a moving bed reactor similar to a FCC type reactor [24]. High acrolein yield (55–61%) was obtained at 350 °C with a HZSM-5-based catalyst (Si/Al = 100, particle size 40–120 μm).

* Corresponding author. Fax: +49 208 306 2995.
E-mail address: schueth@mpi-muelheim.mpg.de (F. Schüth).

0021-9517/$ - see front matter © 2009 Elsevier Inc. All rights reserved.
doi:10.1016/j.jcat.2009.10.017

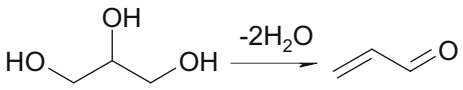

Scheme 1. Double dehydration of glycerol to acrolein.

Nanocrystalline zeolites (<100 nm) could provide large external surface areas and shorten the diffusion distances in the channels of the particles, thereby facilitating access to the active sites and reducing deactivation. There have been some reports on the improved catalytic properties of nanocrystalline ZSM-5, such as increased selectivity in toluene conversion to cresol and decreased coke formation relative to conventional ZSM-5 materials [25]. However, up to now, investigations on the performance of nanocrystalline HZSM-5 catalyst in glycerol dehydration are lacking, although one could expect superior properties compared to materials with larger crystal sizes.

In this paper, we report on investigations on the catalytic behavior of nanocrystalline HZSM-5 with high Si/Al molar ratio (ca. 65) as catalyst for the gas phase dehydration of aqueous glycerol. The results show that, compared with bulk HZSM-5, the corresponding nanocrystalline materials exhibit improved catalytic performance in glycerol dehydration. Besides the size effect, the influence of Si/Al ratio and the proton exchange degree of H_xNa_{1-x}ZSM-5 on the catalytic behavior of the catalyst have also been investigated. Based on the results, we infer that small-sized HZSM-5 with high Al content would be a promising catalyst for gas phase dehydration of glycerol.

2. Experimental sections

2.1. Catalyst preparation

Nanocrystalline zeolite of HZSM-5 (90) was kindly provided by Südchemie (Germany). The number in the bracket is related to the SiO_2/Al_2O_3 molar ratio of different zeolites materials. The actual Si/Al molar ratio for the zeolite may deviate from the gel ratio, it was therefore separately analyzed by EDX attached on a SEM attached to a scanning electron microscope (Table 1).

HZSM-5 (20) was prepared through a cation exchange and calcination process with NaZSM-5 (20) (Südchemie) as starting material. NaZSM-5 was firstly converted to the ammonium form by cation exchange in a NH_4NO_3 solution. Three grams of NaZSM-5 (20) was dispersed in 300 ml NH_4NO_3 solution with a concentration of 1 mol L^{-1} and vigorously stirred for 30 min. The solid products were collected by centrifugation (5000 rpm, 10 min) and redispersed in 300 ml NH_4NO_3 solution with stirring for the second cation exchange. The exchange process was performed altogether 3 times to complete the exchange reaction, and NH_4ZSM-5 (20) was formed. The NH_4ZSM-5 (20) products were washed and collected by centrifugation (5000 rpm, 10 min) for 5 times with distilled water and dried at 80 °C for 12 h. The final H-ZSM-5 (20) product was obtained by calcining the NH_4ZSM-5 (20) powder at 550 °C for 3 h.

HZSM-5 (27) was prepared through the calcination of NH_4ZSM-5 (27) (Südchemie) at 550 °C for 3 h.

The bulk zeolites HZSM-5 (90) and HZSM-5 (200) have been prepared according to the following procedure. The molar composition of the reaction gel was: 4 TPABr:$n$$SiO_2$:$Al(NO_3)_3$:16.5NaOH, 1420$H_2O$, with n = 45 and 100. It has to be noted that not all aluminum present in the reaction gel is incorporated in the final crystallites (see Table 1). NaOH (J.T. Baker) and $Al(NO_3)_3{\cdot}9H_2O$ (Aldrich) were dissolved in 2/5 of the total amount of water. Then Ludox AS30 (Aldrich) was added to that solution. Finally, tetrapropylammonium bromide (TPABr, 98%, Aldrich) dissolved in 3/5 of the total amount of water was added. The resulting gel was homogenized and transferred into Teflon-lined autoclaves and allowed to react at 180 °C for 24 h. The crystalline product was recovered by filtration, washed with deionized water, and dried at room temperature. Calcination was performed at 550 °C for 5 h after heating the as-made zeolite at a heating rate of 2 °C min^{-1} to that temperature. Protonation of the zeolites was achieved as follows. 2 g of calcined zeolite was stirred in 100 mL 1 M NH_4NO_3 solution for 30 min. This procedure was repeated another two times with fresh solutions. The final product was calcined at 550 °C for 3 h.

The silicalite-1 was prepared according to the following procedure. 4.68 g TPAOH (40 wt% in water Aldrich) was added to 5.40 g deionized water under vigorous magnetic stirring. After stirring for 30 min, 5.40 g TEOS (98%, Aldrich) was added and the stirring was continued for 3 h. The resulting white suspension was transferred into Teflon-lined autoclaves and allowed to react at 90 °C for 24 h. The crystalline product was recovered by filtration, washed with deionized water, and dried at 80 °C for 12 h. The organic template was removed by calcination at 550 °C in air. The sample was heated at a rate of 2 °C min^{-1}, and the final temperature was kept for 5 h.

H_xNa_{1-x}ZSM-5 (27) was prepared through a partial cation exchange and calcination process using Na-ZSM-5 (27) (Südchemie) as starting material. Three grams of NaZSM-5 (27) was dispersed in 300 ml solution with certain concentration of ammonium nitrate ($[NH_4NO_3] = 8.6 \times 10^3$ mol L^{-1} for preparing $H_{0.67}Na_{0.33}$ZSM-5 (27), $[NH_4NO_3] = 4.0 \times 10^3$ mol L^{-1} for preparing $H_{0.50}Na_{0.50}$-ZSM-5 (27)) using vigorous stirring for 2 h. The solid product was recovered by centrifugation (5000 rpm, 10 min), washed/centrifuged 5 times with distilled water, and dried at 80 °C for 12 h. The final H_xNa_{1-x}ZSM-5 (27) product was obtained by calcining the $(NH_4)_xNa_{1-x}$ZSM-5 (27) products at 550 °C for 6 h. For comparison HZSM-5 (27) was obtained through a complete cation exchange process, following the same preparation procedure as given above for the synthesis of HZSM-5 (20). To differentiate the samples of H_xNa_{1-x}ZSM-5 (27) from the above HZSM-5 (27) prepared directly through the calcination of commercial NH_4ZSM-5 (27), we label these ZSM-5 (27) samples as ZSM-5 (27)-II in the text below.

Detailed information on all catalysts is given in Table 1. Before use, the catalyst powders were calcined at 350 °C for 5 h, then pressed, crushed, and sieved to 20–40 mesh.

Table 1
Si/Al ratio and particle size of the catalysts used in this study.

Sample	Si/Al molar ratio (EDX result)	SiO_2/Al_2O_3 molar ratio (EDX result)	Particle size
Nanocrystalline HZSM-5 (90)	65	32.5	20-60 nm
Bulk HZSM-5 (90)	64	32	ca. 20 μm
HZSM-5 (20)	14	7	0.3–1 μm × 0.5–3 μm
HZSM-5 (27)	18	9	0.2–2 μm
HZSM-5 (200)	145	72.5	ca. 20 μm
Silicalite-1	$+\infty$	$+\infty$	ca. 300 nm
HZSM-5 (27)-II	17	8.5	ca. 3 μm
$H_{0.67}Na_{0.33}$ZSM-5 (27)-II	17	8.5	ca. 3 μm
$H_{0.50}Na_{0.50}$ZSM-5 (27)-II	17	8.5	ca. 3 μm

2.2. Characterization

The powder X-ray diffraction (XRD) patterns were recorded on a Stoe STADI P diffractometer operating in reflection mode with Cu Kα radiation using a secondary graphite monochromator. Scanning electron microscope (SEM) and energy dispersive X-ray (EDX)

analyses were performed on a Hitachi S-3500 N instrument equipped with an Oxford EDX unit (INCA Surveyor Imaging System). Transmission electron microscope (TEM) images were taken on a Hitachi 7500 transmission electron microscope at a voltage of 100 kV. Thermal analyses (TG-DTA) of the catalyst after reaction, as well as temperature-programmed oxidation (TPO) measurements of the used catalysts, were conducted on a Netzsch STA 449C thermal analyzer. The sample was placed in α-Al_2O_3 crucible and heated in flowing air (40 mL min^{-1}) from room temperature to 800 °C at a rate of 10 °C min^{-1}. The samples were dried overnight at 100 °C before the measurements.

2.3. Catalytic reaction

The gas phase dehydration of glycerol was conducted at 320 °C under atmospheric pressure in a vertical fixed bed reactor (8 mm i.d.) using 1.25 mL of catalyst. Before the reaction, the catalysts were pretreated at 320 °C for 0.5 h in flowing dry N_2 (30 mL min^{-1}). The reaction feed, an aqueous solution containing 35 wt% or 50 wt% glycerol, was fed into the reactor by an Amersham Biosciences piston Pump P-500 at different space velocities (GHSV) of glycerol. The reaction products were condensed in an ice water trap and collected hourly for analysis on a HP5890 gas chromatograph equipped with a DB Wax capillary column (G/496, 15 m long) and a flame ionization detector (FID). The reaction was usually carried out for 10 or 24 h, and the condensed products during the first hour of the reaction were abandoned due to poor material balance. For quantitative determination of the product masses, an internal standard was used. For low boiling point compounds, such as acrolein, allyl alcohol, and 1-hydroxylacetone, 1-propanol was selected as the standard compound. For glycerol, we used 1,2,4-butanetriol as standard compound. The relative mass correction factors (f_i) of the product compounds to the standard compound are shown in Table 2. It is noted that for some products, such as acetaldehyde and propanol, it is difficult to obtain relative mass-correcting factors. Masses of these products were thus calculated using the f_i of acrolein. Due to the low amount of these products formed, this does not strongly affect the quantification of glycerol conversion and acrolein selectivity.

3. Results and discussion

3.1. Characterization and catalytic performance of nanocrystalline HZSM-5 (90)

The commercial nanocrystalline HZSM-5 (90) was provided by Südchemie (Germany). Using powder X-ray diffraction (XRD), scanning electron microscopy (SEM) and Transmission electron microscopy (TEM), structure, morphology and composition of the nanocrystalline HZSM-5 (90) materials were characterized. The XRD analysis proved that the sample was phase pure without amorphous or other crystalline byproducts. The SEM image (Fig. 1) shows the size, particle morphology, and aggregation of the HZSM-5 (90) crystals. The particles form larger agglomerates, which are composed of many smaller individual zeolite particles. Because of the agglomeration of the particles, it is difficult to determine the primary particle size only based on the SEM images. TEM was used to further investigate the microstructure and particle size of the nanocrystalline HZSM-5 (90) catalyst. Fig. 2 shows the TEM images of HZSM-5 (90) at different magnifications. From the TEM images sizes of the primary zeolite particles varying between 20 and 60 nm were determined. The clear lattice fringes visible in Fig. 2d confirm the high crystallinity of the zeolite particles.

Table 2
Relative mass-correcting factor (f_i) for the products for GC quantitative analysis.

Product compound	Standard compound used	Relative mass-correcting factor (f_i)
Acrolein	1-Propanol	1.2
Allyl alcohol	1-Propanol	0.9
1-Hydroxylacetone	1-Propanol	2.1
Glycerol	1,2,4-Butantriol	1.1

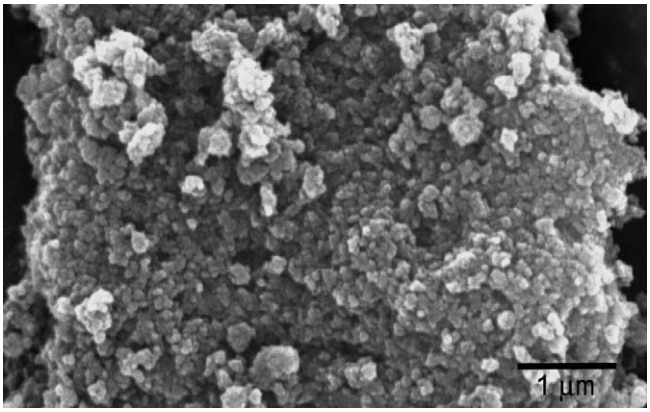

Fig. 1. SEM image of the nanocrystalline HZSM-5 (90).

The catalytic dehydration of glycerol over the HZSM-5 (90) catalyst was firstly conducted with 35 wt% aqueous glycerol. Glycerol conversion and selectivity for acrolein are shown in Fig. 3a. At a gas hourly space velocity (GHSV) of glycerol of 155 h^{-1}, glycerol conversion is always complete at 10 h time on stream (TOS), the selectivity for acrolein increases from 47 mol% at TOS = 2–3 h to 60 mol% at TOS = 9–10 h over the first 10 h. Even at TOS of 23–24 h, the glycerol conversion is still complete. The selectivity for acrolein at TOS = 23–24 h reaches 64 mol%. The full conversion of glycerol and continuously increased selectivity for acrolein demonstrates the high activity of nanocrystalline HZSM-5 (90) for glycerol dehydration. The space velocity of 155 h^{-1} is obviously too low to check whether the catalyst deactivates over 24 h. Space velocity was thus increased to 465 h^{-1}. Glycerol conversion at TOS = 9–10 h was found to be 98% and at TOS = 23–24 h 83%, demonstrating that the catalyst indeed does deactivate to some extent. In order to shorten the experimental time and further study catalyst stability, glycerol concentration was increased to 50 wt% and space velocity was set at 719 h^{-1} or 1438 h^{-1}, respectively. The corresponding catalytic results are shown in Fig. 3b. At a GHSV = 719 h^{-1} which is 12–36 times higher than those (20–60 h^{-1}) documented in patents [6,26,27], the nanocrystalline HZSM-5 (90) still exhibits excellent performance with 83 mol% glycerol conversion and 65 mol% acrolein selectivity at TOS = 9–10 h. Even at GHSV = 1438 h^{-1} and TOS = 9–10 h, high selectivity (67 mol%) and reasonable conversion (57 mol%) is maintained. It is noticed that at GHSV higher than 719 h^{-1}, although the glycerol conversion decreases obviously with the increase of TOS, the selectivity for acrolein is very stable and always higher than 60 mol%.

The product distribution at different GHSV (9–10 h TOS) is shown in Table 3. Acrolein is always the main product and 1-hydroxyacetone resulting from mono dehydration appeared as the main byproduct. Other byproducts identified were acetaldehyde, propanol, and allyl alcohol, all of which with total selectivities usually well below 10 mol% (except GHSV 155 h^{-1} for which a selectivity slightly above 10 mol% was observed). In addition to the identified products listed above, small amounts of other compounds (10–23 mol% estimated by normalization to glycerol reacted assuming a response factor of (1) remained as unidentified products, possibly formed by secondary reactions among products or between product and the reaction feed.

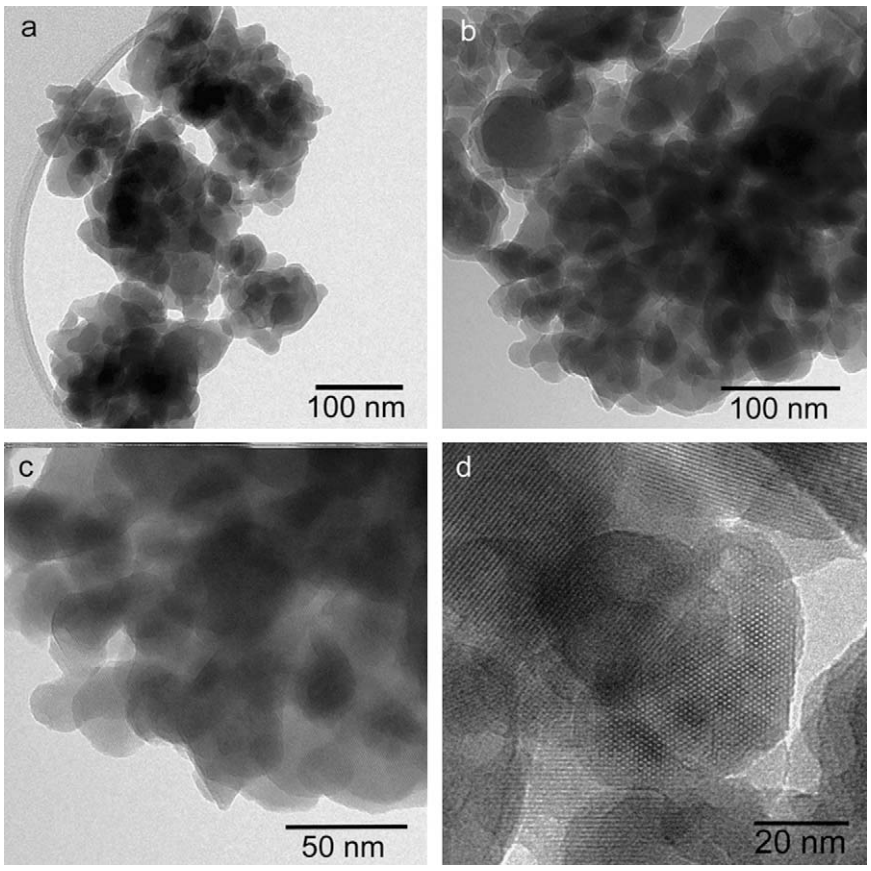

Fig. 2. TEM images of the nanocrystalline HZSM-5 (90) at different magnifications.

Due to the fact that at low space velocities (GHSV $\leqslant$ 719 h^{-1}) conversions reach nearly 100%, the mass normalized productivities increase with increasing GHSV, until a limiting value of around 20 mmol h^{-1} g^{-1} at TOS = 9–10 h (Fig. 4) is reached. At high space velocities (GHSV > 719 h^{-1}), the productivities are limited by the intrinsic activity of the catalyst and the more severe deactivation, which restricts the productivity increase.

The deactivation of the catalyst in glycerol dehydration is normally attributed to carbon deposits formed on the catalyst. Temperature-programmed oxidation (TPO) characterization of the used catalysts (at 24 h TOS) was conducted using flowing air in the TG-DTA instrument; the results are compared in Fig. 5. The weight loss between 320 and 700 °C is accompanied with two exothermic peaks in the DTA curves over the same temperature range, which originates from the oxidation of coke on the used catalyst. The first peak in the DTA curve centered at 360 °C is assigned to the combustion of the carbon deposits that are easily oxidized, e.g. cokes on the outer surface of the catalyst particles and some soft cokes within the micropores, while the second strong peak centered at 517 °C is probably due to the removal of more stable coke in the channel system of the nanocrystalline HZSM-5 (90) [28,29]. The amounts of carbon deposits measured from the TG curves are plotted in Fig. 6 as a function of the GHSV. The general trend is that catalysts at higher GHSV produce more coke than catalysts at lower GHSV. The carbon deposition increases linearly with GHSV from 155 to 719 h^{-1}, while it increases less strongly at GHSV of 1438 h^{-1}, which is well in accordance with the trend of mass-specific rates for glycerol consumption and acrolein formation as shown in Fig. 4.

Attempts were made to regenerate the used nanocrystalline HZSM-5 (90) catalysts by oxidation at elevated temperatures. Calcination of the used catalyst in flowing air is always effective, a simple oxidation treatment with air at the 550 °C for 10 h was found to be sufficient for a full regeneration of the catalysts. The catalytic performance of the catalyst before and after regeneration was almost identical (see Supplementary Fig. S1).

Nanocrystalline zeolites are superior in some applications, because they shorten the diffusion distances in the channels of the particles, expose more external surface sites for reaction, and reduce deactivation. In order to investigate the difference of the catalytic properties between nanocrystalline and bulk HZSM-5, bulk HZSM-5 zeolite (Si/Al = 64, which is almost identical to that of the nanocrystalline material) with a particle size of 20 μm was synthesized and used as catalyst for dehydration of glycerol. Fig. 7 shows the catalytic performance of the bulk HZSM-5 catalyst. Even at low GHSV of 155 h^{-1}, both glycerol conversion and acrolein selectivity are strongly decreased compared to those of the nanocrystalline HZSM-5 zeolite. It can thus be concluded that the particle size of the zeolite catalyst is an important factor determining the catalytic performance in the glycerol dehydration reaction. Brønsted acid sites are assumed to be the more important acid sites for the formation of acrolein by glycerol dehydration [23,30]. For HZSM-5 zeolite, the Brønsted acid sites originate from the charge imbalance by incorporation of Al atom in the Si–O framework. The majority of the structural Brønsted acid sites are located in the channels, only small amounts of Brønsted acid sites are on the outer surface of the zeolite particles. Due to the large particle sizes, mass transfer limitations can be expected for a molecule such as glycerol which reduces the mass-specific productivity of large crystals. In addition, for large crystallites, carbon deposits in the micropores might be preferentially formed in outer region of the particles [31], which could amplify the mass transfer limitations.

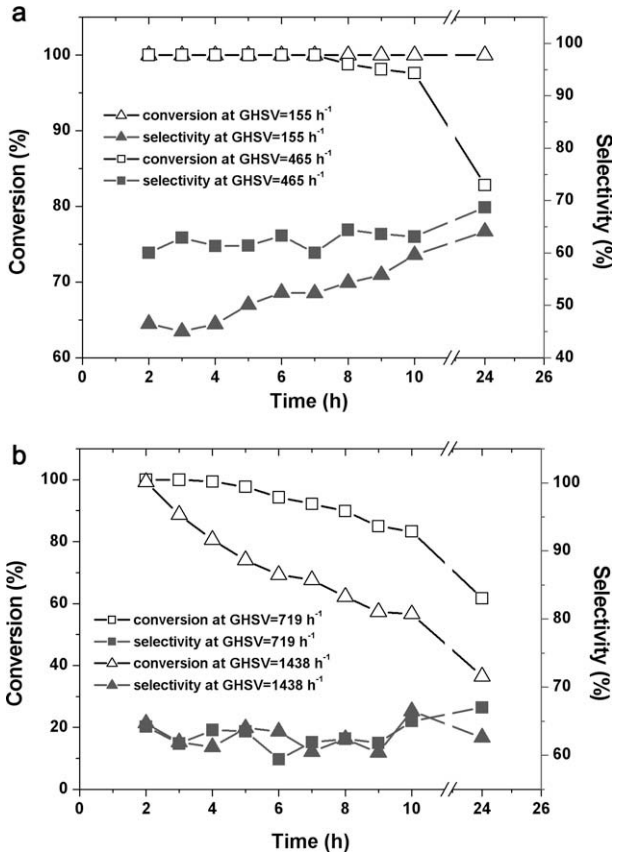

Fig. 3. Glycerol conversion and acrolein selectivity over time for nanocrystalline HZSM-5 (90) catalyst at 320 °C at different GHSV: (a) using 35 wt% glycerol aqueous solution as feed, and (b) using 50 wt% glycerol aqueous solution as feed.

It would be highly attractive to convert not pure aqueous glycerol solutions, but directly the crude glycerol obtained in the transesterification reaction for FAME production. Therefore, also such a feed was used for some of the experiments. The crude glycerol (ca. 80 wt%, provided by Campa Biodiesel company) was diluted to 50 wt% glycerol (otherwise it was too viscous to be pumped efficiently). The catalytic performance of the nanocrystalline HZSM-5 catalyst in the dehydration of diluted crude glycerol is shown in Supplementary Fig. S2. Even with crude glycerol as reactant, the catalyst still exhibits high activity. After 5 h of reaction, the filter of the reactor was blocked and the reaction had to be terminated. However, clogging of a filter is more an engineering problem; the catalyst itself appears to be suitable for the direct conversion of crude aqueous glycerol from FAME production to acrolein.

3.2. Catalytic performance of HZSM-5 catalysts with different Si/Al ratios

Previous studies have shown that Brønsted acid sites are advantageous compared to Lewis acid sites in catalyzing the selective

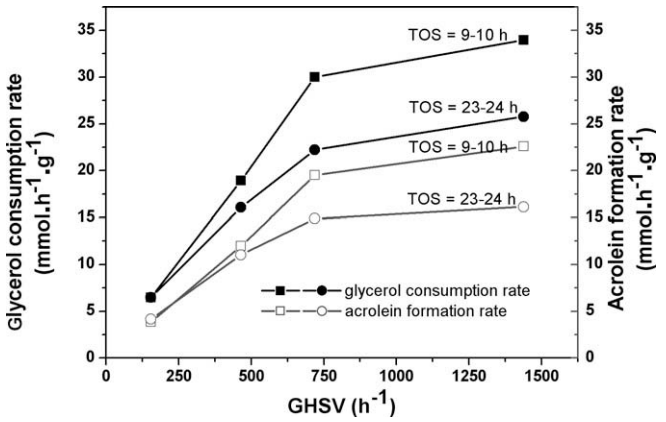

Fig. 4. Mass specific catalytic rates of nanocrystalline HZSM-5 (90) catalysts for glycerol conversion and acrolein formation at TOS = 9–10 h and 23–24 h at different GHSV.

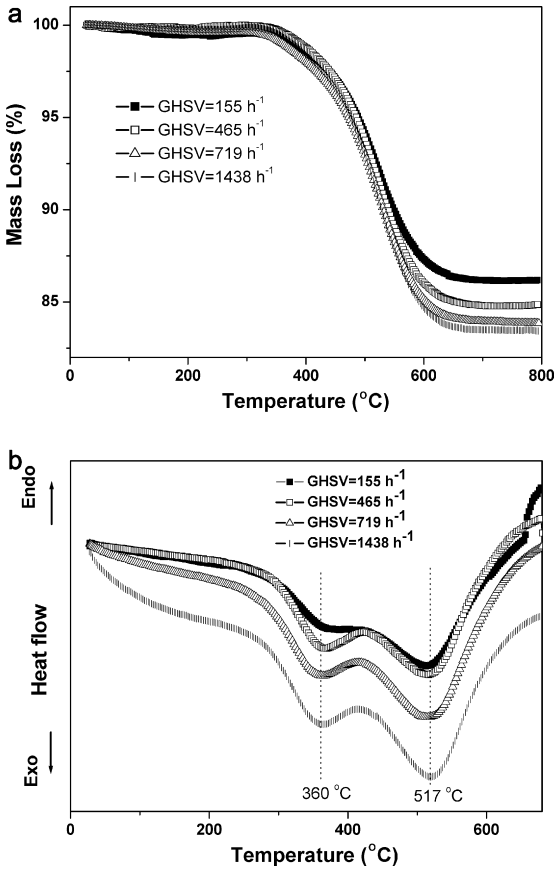

Fig. 5. (a) TG, and (b) DTA curves of the nanocrystalline HZSM-5 (90) catalysts after reaction at different GHSV.

Table 3
Product distribution over nanocrystalline HZSM-5 (90) catalyst with different GHSV (TOS = 9–10 h).

GHSV (h^{-1})	Conversion (mol%)	Product selectivity (mol%)					
		Acrolein	Acetaldehyde	Allyl alcohol	Propanol	1-Hydroxyacetone	Others
155	100	60	11	0	3	5	21
465	98	63	6	0	2	6	23
719	83	65	7	3	2	11	12
1438	57	67	8	2	1	12	10

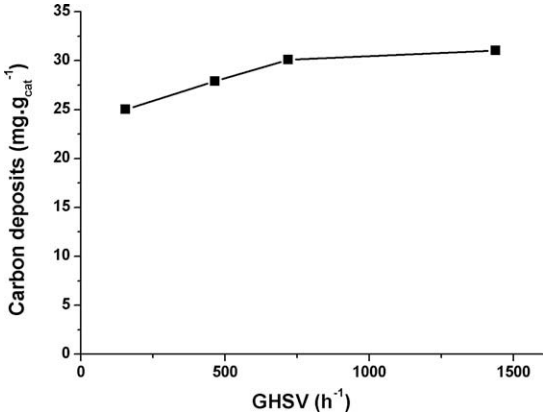

Fig. 6. Effect of space velocity on the amount of carbon deposits over the used nanocrystalline HZSM-5 catalysts (90) (TOS = 23–24 h).

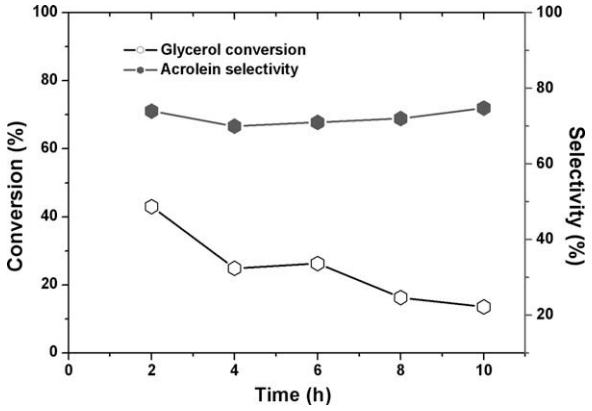

Fig. 7. Time course of glycerol conversion and acrolein selectivity over bulk HZSM-5 (90) catalyst using aqueous solution with 35 wt% glycerol as feed at GHSV = 155 h^{-1}.

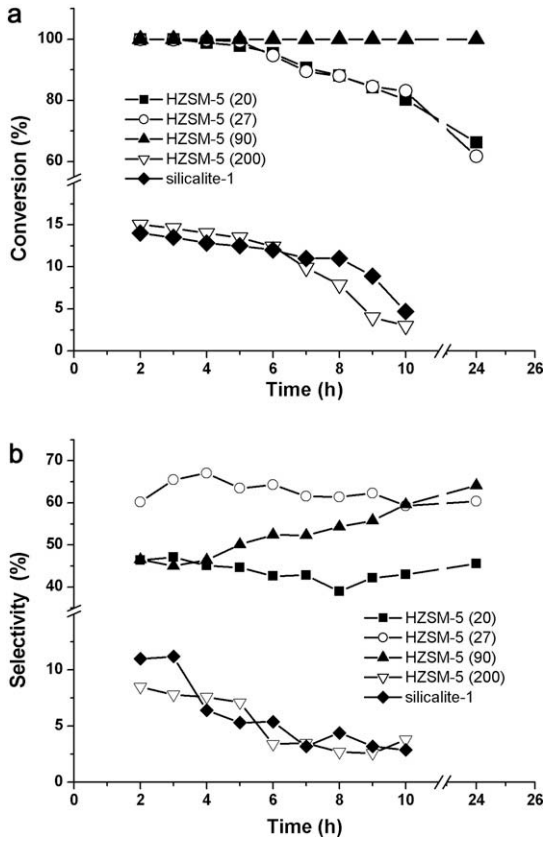

Fig. 8. Time course of: (a) glycerol conversion, and (b) acrolein selectivity over HZSM-5 catalyst with different Si/Al molar ratios.

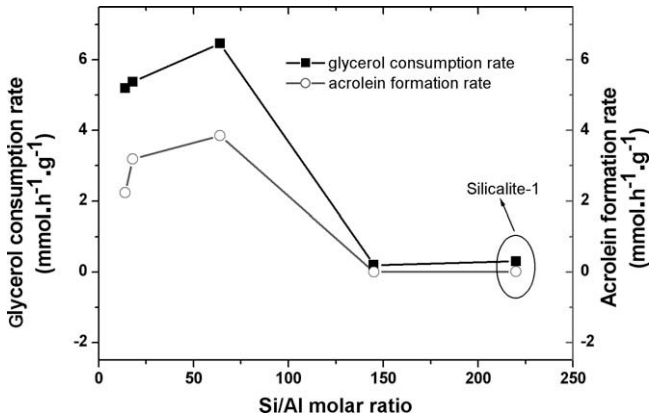

Fig. 9. Mass specific catalytic rates of over HZSM-5 catalysts with different Si/Al molar ratios for glycerol conversion and acrolein formation at TOS = 9–10 h.

synthesis of acrolein from glycerol [23,30]. For HZSM-5, the strong Brønsted acidity of bridging Si–(OH)–Al sites is generated by the presence of aluminum in the silicate framework, and the density of the Brønsted acid sites is directly determined by the aluminum content. Therefore, it is expected that the variation of the Si/Al molar ratio will affect the catalytic performance of HZSM-5 zeolites in glycerol dehydration. The effect of Si/Al molar ratio on the surface properties of HZSM-5 zeolites and catalytic performance has been studied for many reactions [32–34], but up to now, there is no report on the effect of Si/Al molar ratio on the catalytic performance of HZSM-5 in glycerol dehydration. Thus, HZSM-5 zeolites with different Si/Al molar ratios (Si/Al = 14, 18, 65, 145) and Silicalite-1 were studied in the production of acrolein by glycerol dehydration.

Glycerol conversion and acrolein selectivity after different TOS and GHSV = 155 h^{-1} are shown in Fig. 8a and b. Based on the data at TOS = 9–10 h, the corresponding mass-specific rates for glycerol consumption and acrolein formation were calculated (see Fig. 9). Both, rates for glycerol consumption and acrolein formation, increase in the range of Si/Al = 14–65, then decrease from Si/Al = 65 to ∞ (Silicalite-1). At first sight, it appears as if the performance of the HZSM-5 reaches a peak around Si/Al = 65. However, if one analyzes the particle size of the catalysts with different Si/Al molar ratios using SEM, it was found that they are quite different (Fig. 10). Particle size of the HZSM-5 (90) lies between 20 to 60 nm (Fig. 2). The commercial HZSM-5 (20) catalyst exhibits rod-like morphology with rod diameters of 0.3–1 μm and lengths of 0.5–3 μm. For the commercial HZSM-5 (27) catalyst, most particles are in the micrometer size range bigger than 1 μm. The HZSM-5 (200) catalyst that we synthesized consists of spherical particles with diameters of about 20 μm, while the Silicalite-1 particles, also exhibiting spherical morphology, have diameters of ca 300 nm. Thus, the particle sizes of the different catalysts change strongly with the variation of the Si/Al molar ratio. Knowing that the reaction suffers from mass transfer limitation in the zeolite channel system (see above), the trends described can not unequivocally be ascribed to the Si/Al ratio. We have made numerous attempts to synthesize a sample set with identical particle sizes, but Si/Al ra-

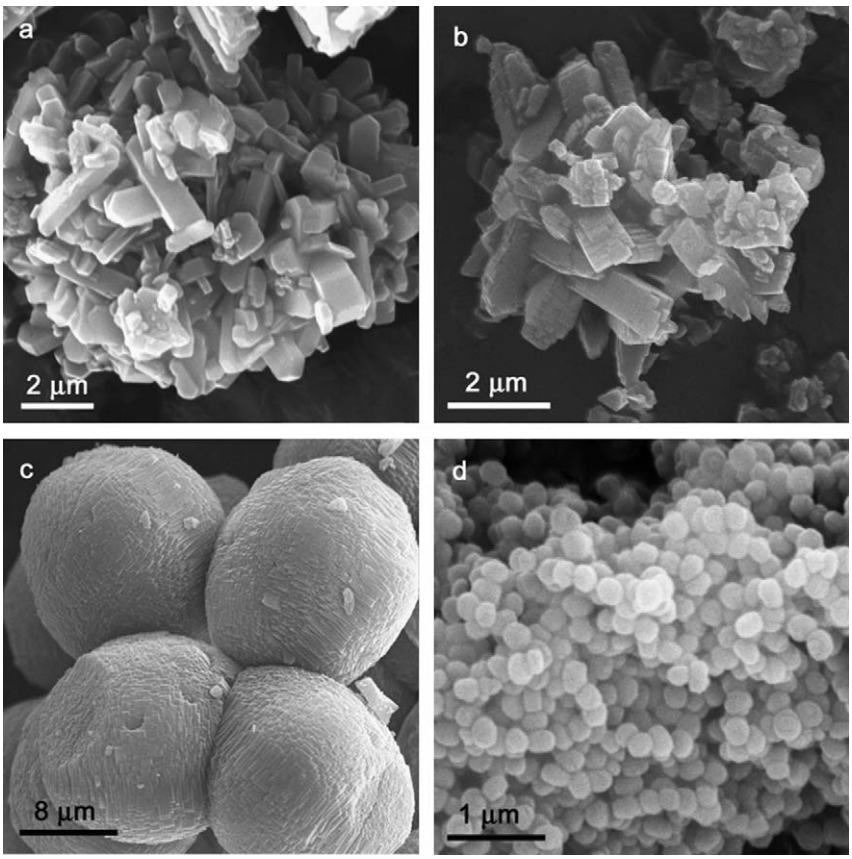

Fig. 10. SEM images of HZSM-5 catalysts with different Si/Al molar ratios: (a) HZSM-5 (20), (b) HZSM-5 (27), (c) HZSM-5 (200), and (d) silicalite-1.

tios differ over a wide range. However, up to now these attempts were unsuccessful. Therefore, NaZSM-5 from one batch has been partially protonated to different degrees. In this way the density of Brønsted sites has been varied but the particle sizes were kept identical.

3.3. Catalytic performance of H_xNa_{1-x}ZSM–5 catalysts

For the synthesis of HZSM-5 zeolite, normally NaZSM-5 is prepared in a first step, and zeolites with other counter ions are obtained via a corresponding ion exchange process. HZSM-5 is prepared by calcining NH_4ZSM-5 results from ammonium exchange of NaZSM-5. In this study $(NH_4)_xNa_{1-x}$ZSM-5 ($0 \leqslant x \leqslant 1$) has been obtained by partial ammonia exchange, successive calcination led to H_xNa_{1-x}ZSM-5. Since the particle sizes did not change significantly during the ion exchange process, the density of the Brønsted acid sites has been varied by tuning the ratio of H/Na in the H_xNa_{1-x}ZSM–5 with fixed Si/Al ratio. Compared to tuning the Si/Al molar ratio during synthesis, partially replacing Na^+ in NaZSM-5 with protons provides a simpler way to synthesize a series of catalysts with different densities of Brønsted acid sites and identical particle sizes.

Accordingly a series of H_xNa_{1-x}ZSM-5 (27)-II (x = 0.50, 0.67 and 1) was prepared by calcining the corresponding $(NH_4)_xNa_{1-x}$ZSM-5 which were obtained through partial ammonia exchange of commercial NaZSM-5 (27) (Südchemie). The sodium concentrations of the zeolites were determined by EDX analyses; values of x = 0.50, 0.67, and 1.0 were found. Since the ion exchange could result in inhomogeneous H^+/Na^+ profiles throughout a zeolite batch, the sodium distribution over the batches was analyzed. Fig. 11 shows the element mapping results of H_xNa_{1-x}ZSM-5 (27)-II (x = 0.50 and 0.67). The Na distribution in the sample is homogeneous, indicating that the Brønsted acidic bridging Si–(OH)–Al sites are also homogeneously distributed in the catalyst. The catalytic performance for glycerol dehydration of the different samples in the series H_xNa_{1-x}ZSM-5 (27)-II (x = 0.50, 0.67, and 1.0) is shown in Fig. 12. It improves with decrease of the Na^+ content in H_xNa_{1-x}ZSM-5 (27)-II, and fully proton-exchanged HZSM–5 (27)-II exhibits the highest activity. Na^+ is supposed to be inactive for alcohol dehydration [35], and the effect of Na^+ on mass transfer in the channel system of ZSM-5 is probably negligible. It can thus be concluded that the concentration of Brønsted acid sites favors both glycerol conversion and acrolein production for H_xNa_{1-x}-ZSM–5 (27)-II catalysts. A similar phenomenon was also found in another reaction system using HY zeolite as the catalyst [36].

The results of this study thus provide a recipe for optimizing ZSM-5 zeolites for glycerol dehydration: small-sized HZSM-5 with low Si/Al ratio seems to be optimal for this reaction. It is advantageous with respect to two points, high density of Brønsted acid sites and enhanced mass transfer in the channel system of the zeolite. However, there are only few reports on the synthesis of small-sized ZSM-5 zeolites with low Si/Al molar ratio, and typically Al^{3+} is not homogeneously distributed in the framework of individual zeolite crystallites. Aluminum might be even present in form of amorphous species to some extent [37]. This complicates the investigation of the catalytic performance of these materials due to the diversity of the local aluminum coordination environment. The challenge for the future is therefore the synthesis of nanosized ZSM-5 zeolites with low Si/Al ratio and full incorporation of aluminum in the zeolite framework.

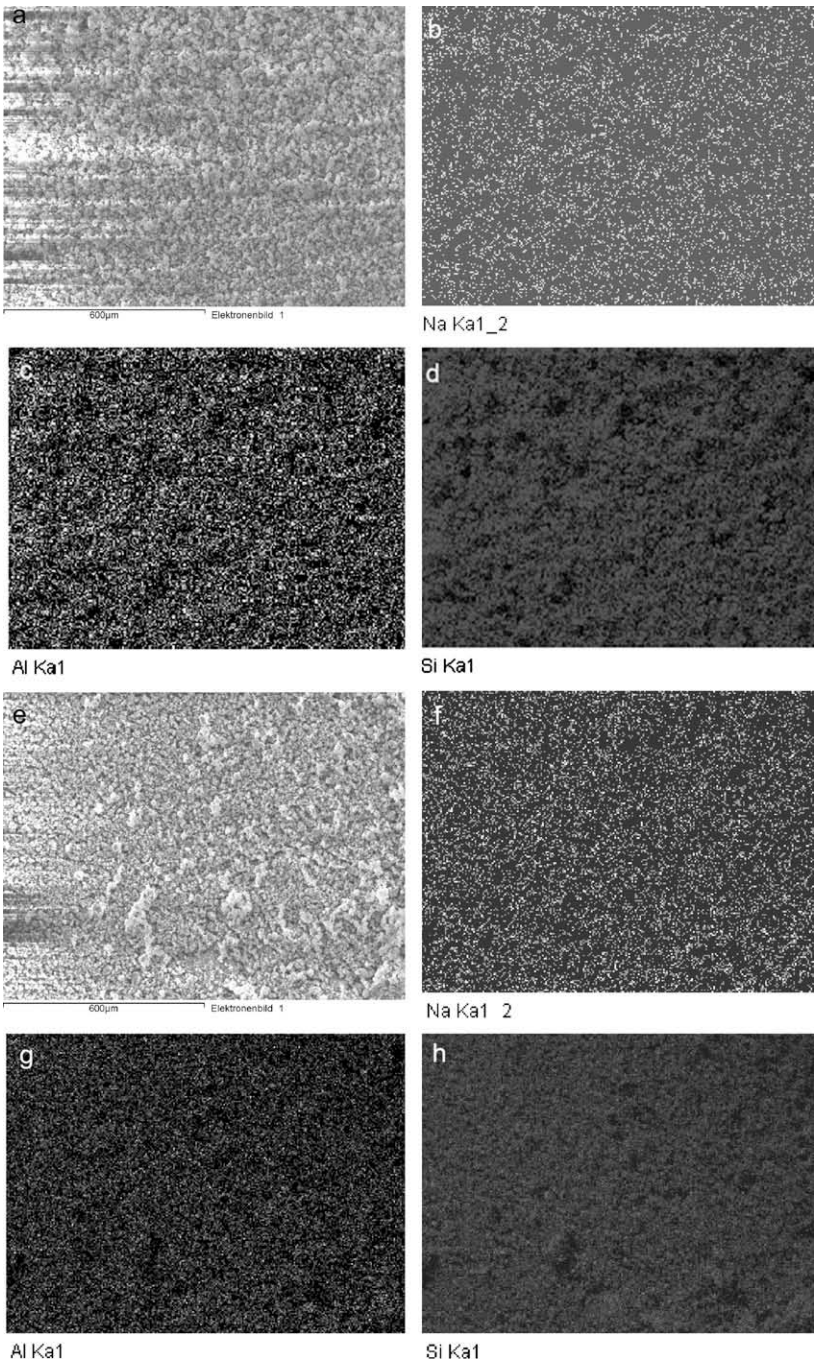

Fig. 11. SEM image and element mapping of $H_{0.50}Na_{0.50}$ZSM-5 (27)-II and $H_{0.67}Na_{0.33}$ZSM-5 (27)-II. (a) normal SEM image, (b) Na mapping, (c) Al mapping, (d) Si mapping for $H_{0.50}Na_{0.50}$ZSM-5 (27)-II, (e) normal SEM image, (f) Na mapping, (g) Al mapping, and (h) Si mapping for $H_{0.67}Na_{0.33}$ZSM-5 (27)-II.

4. Conclusion

We investigated the catalytic behavior of nanocrystalline HZSM-5 catalyst with a Si/Al ratio of 65 for the gas phase dehydration of aqueous glycerol. Compared to bulk HZSM-5, the small-sized catalyst exhibits strongly enhanced catalytic performance in glycerol dehydration even at very high space velocity (GHSV = 1438 h^{-1}). The materials showed promising productivities even with crude glycerol directly from Biodiesel production as feed. The influence of the Si/Al molar ratio of HZSM-5 on the catalytic behavior cannot be easily determined due to the variation of the particle sizes of different catalysts and the fact that mass transfer plays an important role in this reaction. By controlling the proton exchange degree in H_xNa_{1-x}ZSM-5, we prepared a series of HZSM-5 catalysts with identical particle size and different Brønsted acid site densities. The catalytic results show that a high density of Brønsted acid sites favors the production of acrolein. Based on the results of these studies, one can conclude that small-sized HZSM-5 with high Al content should be a promising catalyst for the gas phase dehydration of glycerol due to its advantages in both high Brønsted acid site density and good mass transfer in the channel system of the zeolite.

Acknowledgments

We thank Dr. C. Lehmann, Mrs. S. Palm, and Mr. A. Dreier for the SEM and TEM measurement, Mr. U. Häusig, Mr. F. Kohler, and Ms. C. Heidgen for the GC measurement and analysis.

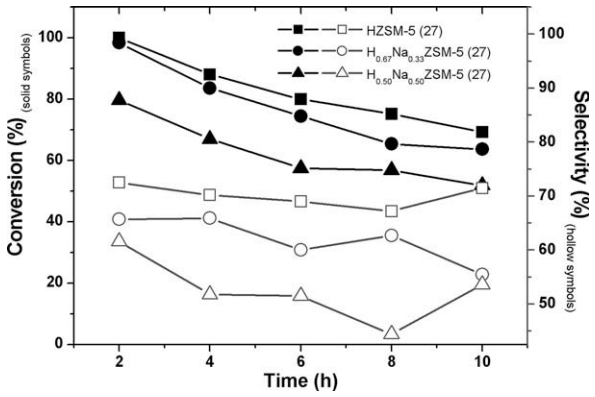

Fig. 12. Time course of glycerol conversion and acrolein selectivity over H_xNa_{1-x}ZSM-5 (x = 0.50, 0.67 and 1) (27)-II catalysts at GHSV = 239 h^{-1} (using 50 wt% glycerol aqueous solution as feed).

Funding, in addition to basic support by the Max Planck Society, was provided by the Leibniz award of DFG and the Alexander von Humboldt Foundation.

Appendix A. Supplementary material

Supplementary data associated with this article can be found, in the online version, at doi:10.1016/j.jcat.2009.10.017.

References

[1] I. Diaz, C. Marquez-Alvarez, F. Mohino, J. Perez-Pariente, E. Sastre, J. Catal. 193 (2000) 295.
[2] T. Miyazawa, Y. Kusunoki, K. Kunimori, K. Tomishige, J. Catal. 240 (2006) 213.
[3] J.M. Clacens, Y. Pouilloux, J. Barrault, Appl. Catal. A 227 (2002) 181.
[4] M.M. Azam, A. Waris, N.M. Nahar, Biomass Bioenergy 29 (2005) 293.
[5] H. Adkins, W.H. Hartung, Org. Synth. Coll. 1 (1941) 15.
[6] A. Neher, T. Haas, D. Arntz, H. Klenk, W. Girke, US Patent 5 387 720, 1995, to Degussa Aktiengesellschaft.
[7] E. Schwenk, M. Gehrke, F. Aichner, US Patent 1 916 743, 1933, to Scheering-Kahlbaum.
[8] S.-H. Chai, H.-P. Wang, Y. Liang, B.-Q. Xu, Appl. Catal. A 353 (2009) 213.
[9] S.-H. Chai, H.-P. Wang, Y. Liang, B.-Q. Xu, Green Chem. 10 (2008) 1087.
[10] H. Atia, U. Armbruster, A. Martin, J. Catal. 258 (2008) 71.
[11] E. Tsukuda, S. Sato, R. Takahashi, T. Sodesawa, Catal. Commun. 8 (2007) 1349.
[12] L.L. Ning, Y.J. Ding, W.M. Chen, L.F. Gong, R.H. Lin, Y. Lu, Q. Xin, Chin. J. Catal. 29 (2008) 212.
[13] S. Ramayya, A. Brittain, C. DeAlmeida, W. Mok, M.J. Antal, Fuel 66 (1987) 1364.
[14] M.J. Antal Jr., W.S.L. Mok, G.N. Richards, Carbohyd. Res. 199 (1990) 111.
[15] W. Buhler, E. Dinjus, H.J. Ederer, A. Kruse, C. Mas, J. Supercrit. Fluid 22 (2002) 37.
[16] L. Ott, M. Bicker, H. Vogel, Green Chem. 8 (2006) 214.
[17] M. Watanabe, T. Iida, Y. Aizawa, T.M. Aida, H. Inomata, Bioresour. Technol. 98 (2007) 1285.
[18] C.H. Baerlocher, W.M. Meier, D.H. Olson, Atlas of Zeolite Framework Types, fifth ed., Elsevier Science, Amsterdam, 2001.
[19] D.W. Breck, Zeolite Molecular Sieves: Structure, Chemistry, and Use, Wiley-Interscience, New York, 1974.
[20] F. Schüth, K.S.W. Sing, J. Weitkamp (Eds.), Handbook of Porous Solids, Wiley-VCH, Weinheim, 2007.
[21] K. Rajagopalan, G.W. Young, Hydrocarbon cracking selectivities with a dual zeolite fluid cracking catalyst containing REY and ZSM-5, Prepr. Am. Chem. Soc., Div. Pet. Chem. 32 (1987) 627.
[22] J. Biswas, I.E. Maxwell, Octane enhancement in fluid catalytic cracking. I. Role of ZSM-5 addition and reactor temperature, Appl. Catal. 58 (1990) 1.
[23] S.-H. Chai, H.-P. Wang, Y. Liang, B.-Q. Xu, Green Chem. 9 (2007) 1130.
[24] A. Corma, G.W. Huber, L. Sauvanaud, P. O'Connor, J. Catal. 257 (2008) 163.
[25] B. Vogel, C. Schneider, E. Klemm, Catal. Lett. 79 (2002) 107.
[26] E. Schwenk, M. Gehrke, F. Aichner, US Patent 1,916,743, 1933, to Scheering-Kahlbaum A.-G.
[27] U.-L. Dubois, C. Duquenne, W. Holderlich, WO Patent 2006/087083 A2, 2006, to Alkema.
[28] A. Hassan, A. Sayari, Appl. Catal. A 297 (2005) 159.
[29] X.J. Zhang, Y. Wang, F. Xin, Appl. Catal. A 307 (2006) 222.
[30] S.H. Chai, H.P. Wang, Y. Liang, B.Q. Xu, J. Catal. 250 (2007) 342.
[31] D. Mores, E. Stavitski, M.H.F. Kox, J. Kornatowski, U. Olsbye, B.M. Weckhuysen, Chem. Eur. J. 14 (2008) 11320.
[32] V.R. Choudhary, V.S. Nayak, Zeolites 5 (1985) 325.
[33] M.A. Ali, B. Brisdon, W.J. Thomas, Appl. Catal. A 252 (2003) 149.
[34] C.S. Triantafillidis, N.P.E. Nalbandian, I.A. Vasalos, Ind. Eng. Chem. Res. 38 (1999) 916.
[35] M.T. Xu, J.H. Lunsford, D.W. Goodman, A. Bhattacharyya, Appl. Catal. A 149 (1997) 289.
[36] Y. Morita, T. Kimura, F. Kato, M. Tamagawa, Bull. Jpn. Petrol. Inst. 14 (1972) 192.
[37] S. Frisch, L.M. Rösken, J. Caro, M. Wark, Micropor. Mesopor. Mater. 120 (2009) 47.